Jeong–Spectral aerosol properties (330–800 nm) from SMART–s

Ukkyo Jeong, University of Maryland / ESSIC (and SMARTLabs of NASA / GSFC)
Si-Chee Tsay, NASA / GSFC, and **many collaborators (Pandora, AERONET, RCL, NIER, ...)**

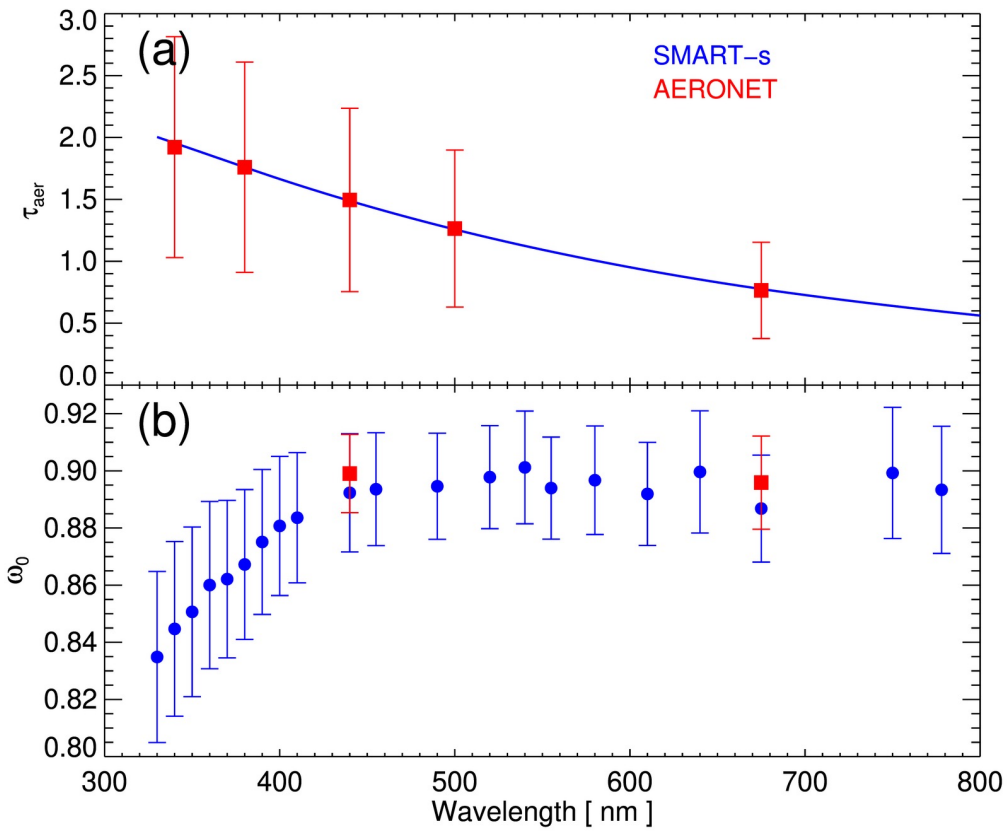

Mean values of (a) spectral aerosol optical thickness (τ_{aer}) and (b) Single-scattering albedo (ω_0) from SMART–s (blue) and AERONET (red) within SMART–s spectral range measured from 8 March to 2 May 2019 at Fang, Thailand: (Jeong et al., 2021, *under preparation*)

Full title: High spectral-resolution of aerosol optical properties from 330 to 800 nm retrieved from extended-range Pandora (SMART–s: Spectral Measurements for Atmospheric Radiative Transfer–spectroradiometer) for ancillary information of trace gas algorithms

Radiometric calibration

Combination of laboratory calibration (at RCL of NASA/GSFC), Langley calibration, and reference solar spectrum

Inversion algorithm

Optimal-estimation based scheme provides: Aerosol size, complex refractive index, single scattering albedo, aerosol optical depth with averaging kernel and solution error of each retrieval

Field studies including comparison/validation efforts

Biomass-burning aerosols at Fang (Thailand), Urban background aerosols over NASA/GSFC (USA), Mixed aerosols over Seosan (Korea)

Future plans/applications

For more details and/or data contact: ukkyo.jeong@nasa.gov or si-chee.tsay-1@nasa.gov

High spectral-resolution of aerosol optical properties from 330 to 800 nm retrieved from extended-range Pandora (SMART–s) for ancillary information of trace gas algorithms

Ukkyo Jeong (UMD / ESSIC), Si-Chee Tsay (NASA / GSFC), and **many collaborators (Pandora, AERONET, RCL, NIER, ...)**

Radiometric calibration

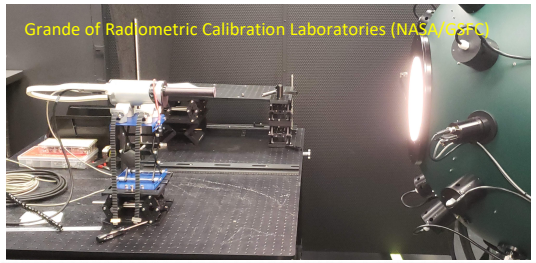

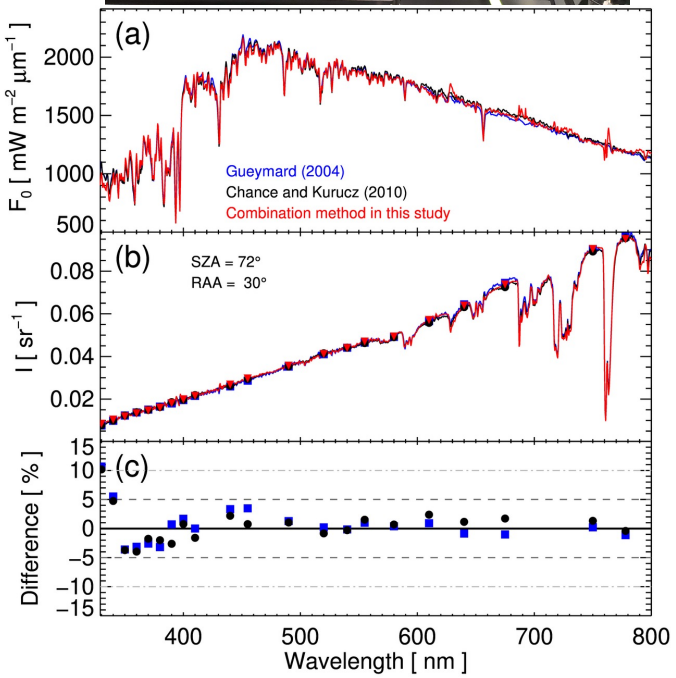

Combination of laboratory calibration, Langley calibration, and reference solar spectrum (Chance and Kurucz, 2010)

Accuracy of the sky radiance **~ 5% in the UV and ~3% in the visible/NIF**

Inversion algorithm

Parameter index	Parameter
1	Mean radius of fine mode (r_f)
2	Geometric standard deviation of fine mode (σ_f)
3	Mean radius of coarse mode (r_c)
4	Geometric standard deviation of coarse mode (σ_c)
5	Number fine-mode fraction (F_{num})
6	Peak height of the aerosol (z_p)
7	Half width of the aerosol layer (h)
Next n Wavelengths	Fine-mode real refractive index (n_f)
Next n Wavelengths	Coarse-mode real refractive index (n_c)
Next n Wavelengths	Fine-mode imaginary refractive index (k_f)
Next n Wavelengths	Coarse-mode imaginary refractive index (k_c)
Next n Wavelengths	Lambertian surface albedo (ρ)

Optimal-estimation based scheme provides: **Aerosol optical depth**, **single scattering albedo**, **particle size**, **complex refractive index**, with **Averaging Kernel** and **Solution Error** of **Each Retrieval**

Details are at Jeong et al. (2020)

SSA comparison

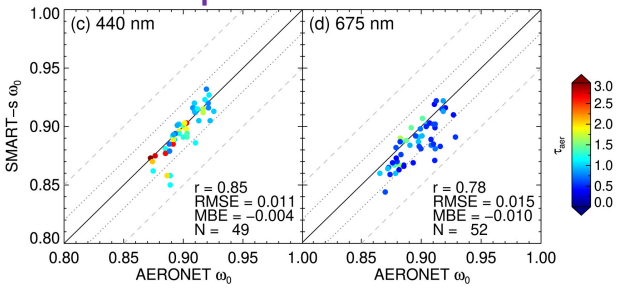

PSD comparison

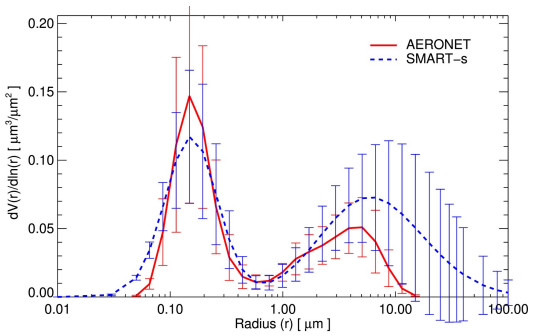

Fang, Thailand Retrievals

March–April 2019 (**Biomass Burning** aerosols)

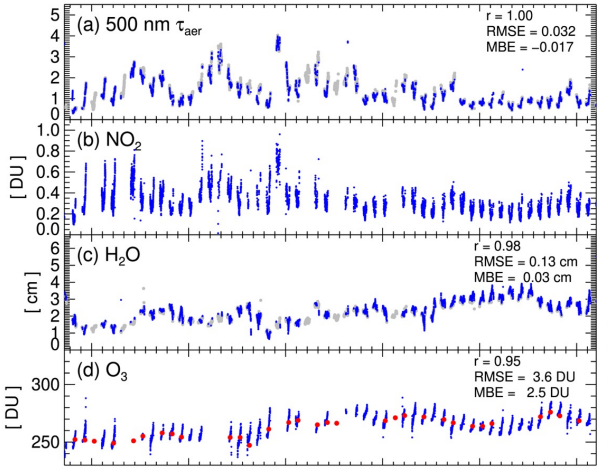

Spectral aerosol properties

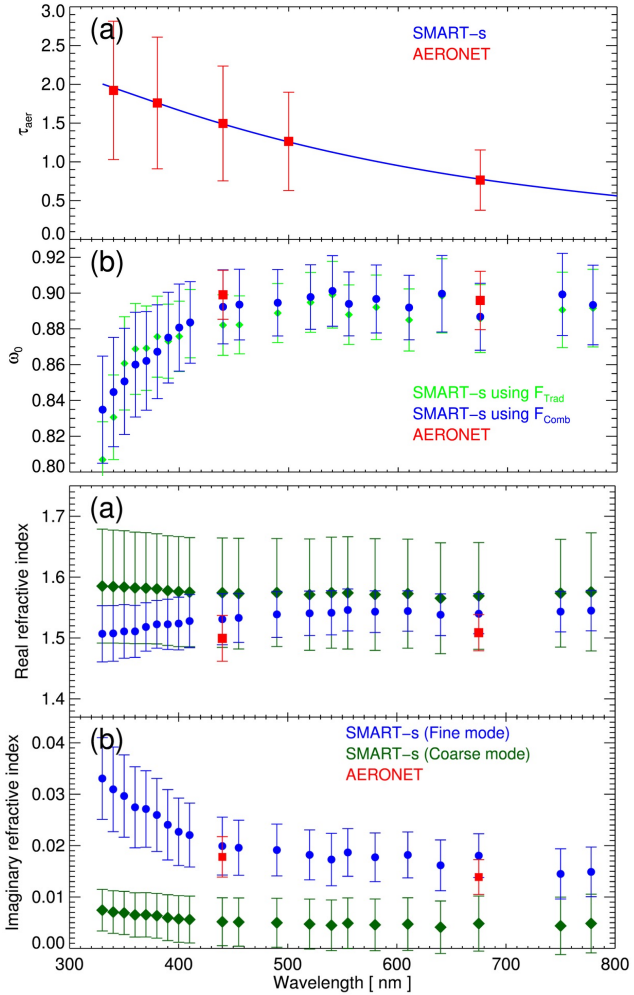

Radiometric Calibration

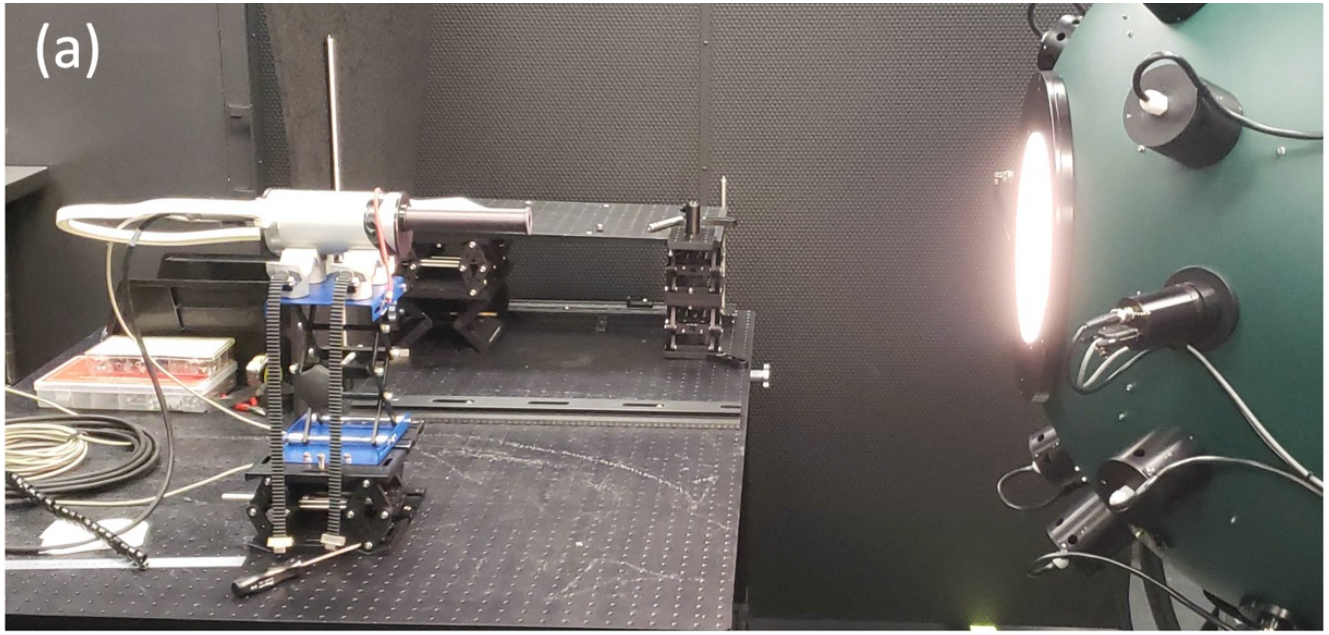

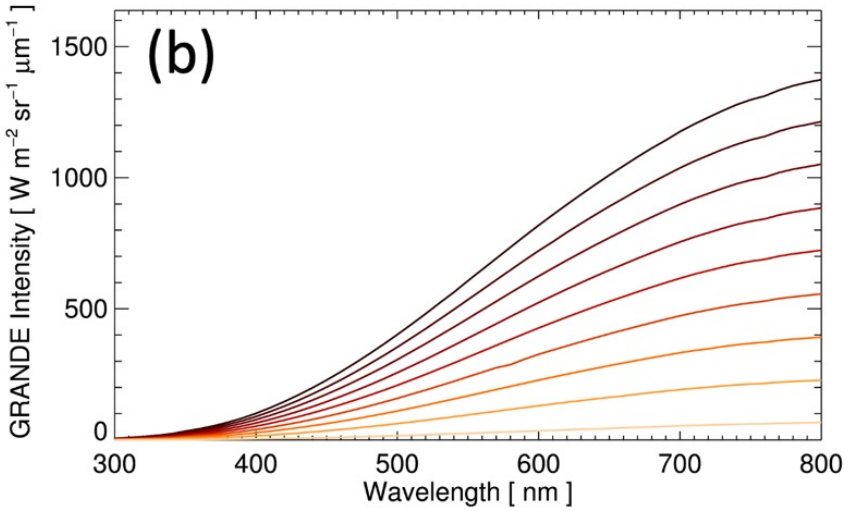

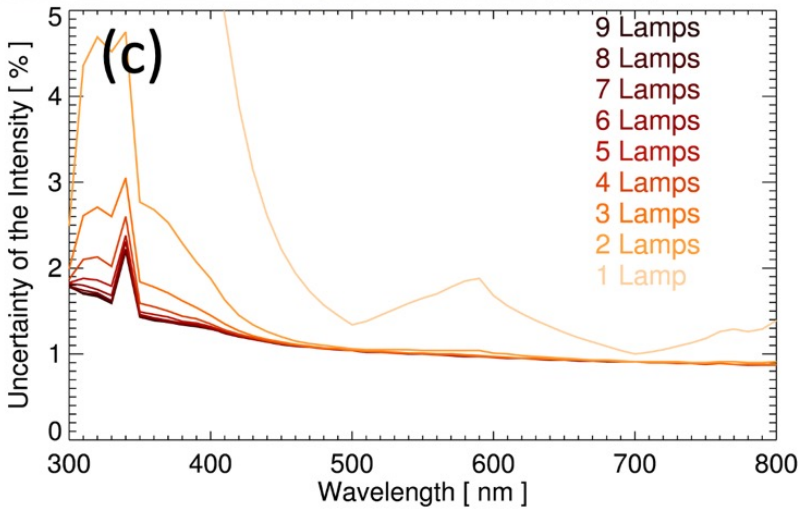

(a) Image of SMART–s calibration using NIST-traceable light source (Grande) of Radiometric Calibration Laboratory at NASA Goddard Space Flight Center. Panel (b) shows spectral intensity of the Grande in the SMART–s spectral range, and panel (c) presents its reported uncertainty. Different colors in (b) and (c) indicate nine levels of the Grande intensity.

Radiometric Calibration

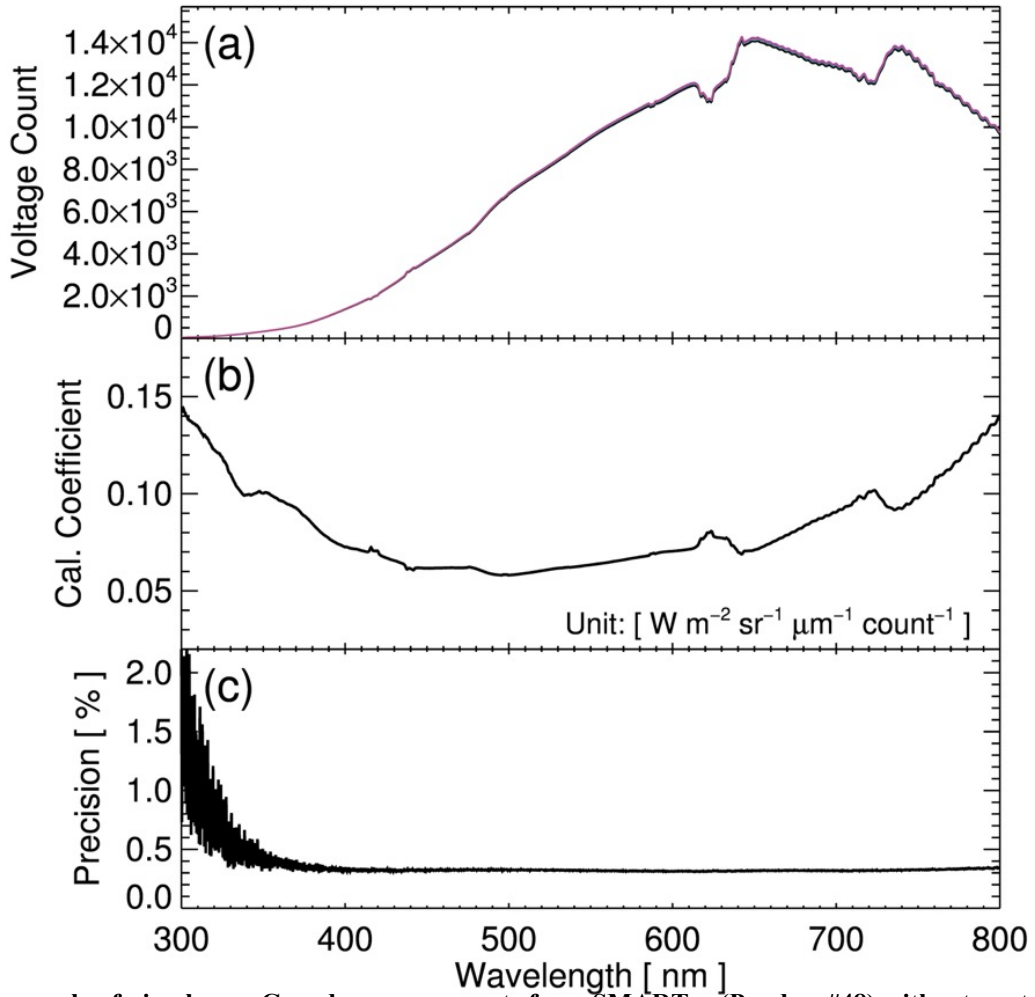

(a) An example of nine-lamps Grande measurements from SMART–s (Pandora#48) without neutral density or band-pass filters. Different colors indicate ten times of repetitions, which overlap almost on top of each other. Panel (b) is calibration coefficient, which is calculated from dividing known Grande intensity by average value of the measured voltage count. (c) is precision of the calibration coefficient, which is estimated by calculating standard deviation of the ten times of repetitions.

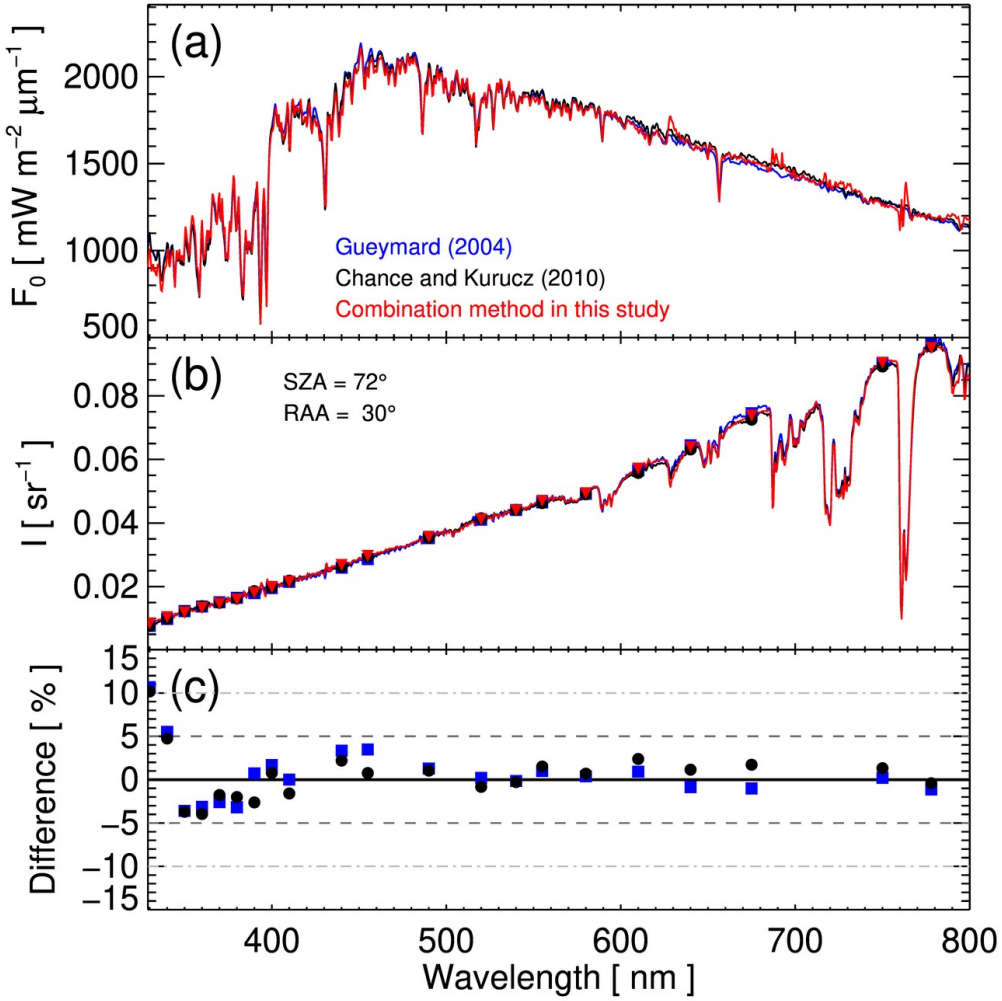

(a) Spectral solar irradiances (F_0) from Gueymard, 2004 (blue), Chance and Kurucz, 2010 (black), and suggested method in this study (red). Panel (b) is an example of converted normalized radiance (radiance divided by solar irradiance, F_0) measured at Fang, Thailand on 19 March 2019. Color of line indicates different sources of F_0 for the conversion (same as in panel a), and circles, triangles, and rectangles depict selected wavelengths of aerosol inversion in this study. Panel (c) presents relative biases of the F_L compared to the Gueymard, 2004 (blue rectangle) and Chance and Kurucz, 2010 (black circle).

Inversion Algorithm

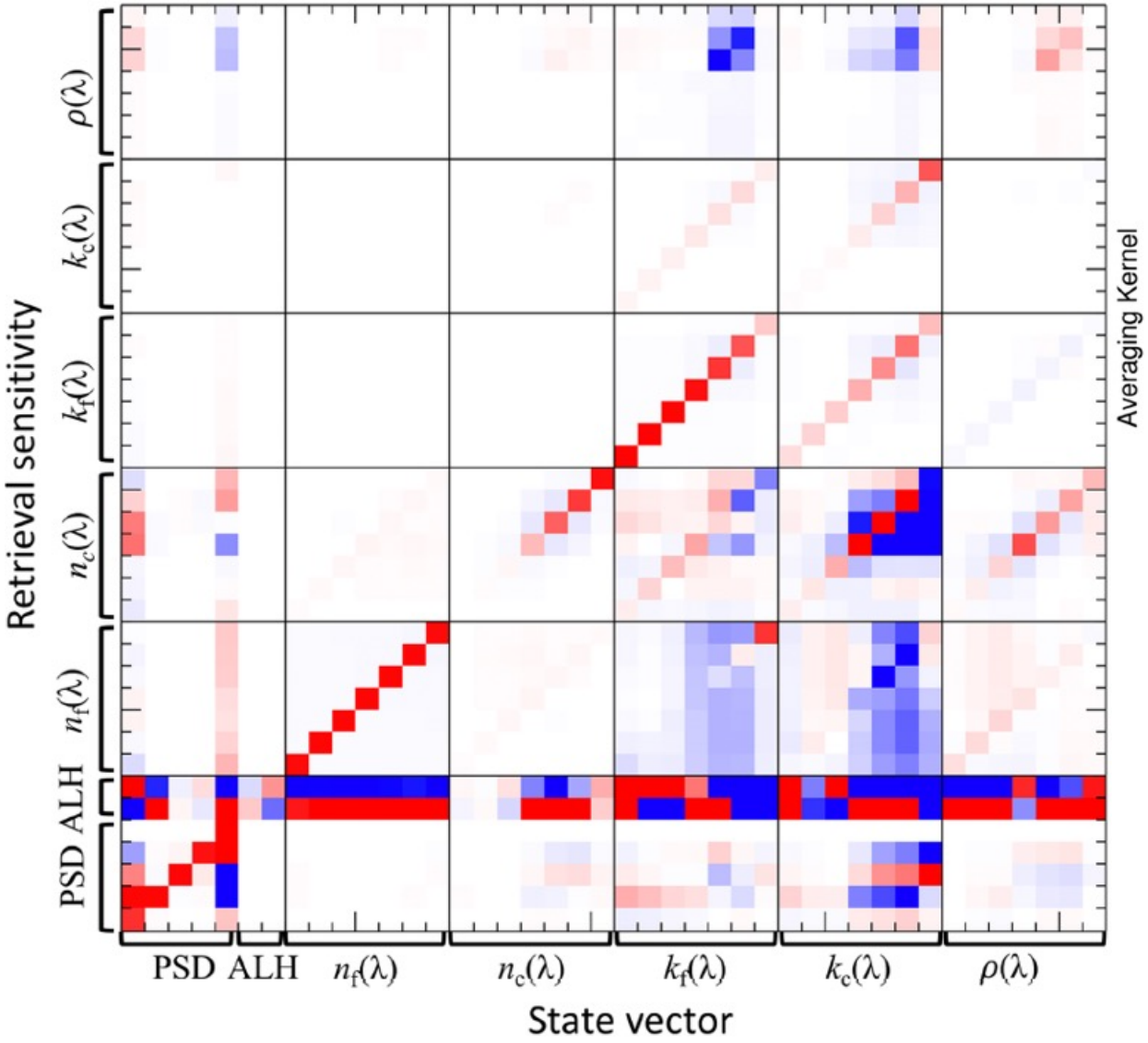

Jeong et al. (2020), *JGR-Atmosphere*

Averaging kernel matrix

This example is for smoke aerosols (fine-mode dominated, moderately absorbing) at SZA of 60°, using the AERONET-like measurements (wavelengths at 380, 440, 500, 675, 870, 1020, and 1640 nm).

The SMART-s algorithm was applied to year-long AERONET data (Sun and sky radiances) measured at **Kanpur (India) and Seoul (South Korea) in 2016,** for consistency check.

Parameter index	Parameter
1	Mean radius of fine mode (r_f)
2	Geometric standard deviation of fine mode (σ_f)
3	Mean radius of coarse mode (r_c)
4	Geometric standard deviation of coarse mode (σ_c)
5	Number fine-mode fraction (F_{num})
6	Peak height of the aerosol (z_p)
7	Half width of the aerosol layer (h)
Next n Wavelengths	Fine-mode real refractive index (n_f)
Next n Wavelengths	Coarse-mode real refractive index (n_c)
Next n Wavelengths	Fine-mode imaginary refractive index (k_f)
Next n Wavelengths	Coarse-mode imaginary refractive index (k_c)
Next n Wavelengths	Lambertian surface albedo (ρ)

Consistency check with the AERONET

SSA retrievals at shorter wavelengths were more consistent between the two algorithms due to the higher AOT

Iterative fitting example (2 January 2016)

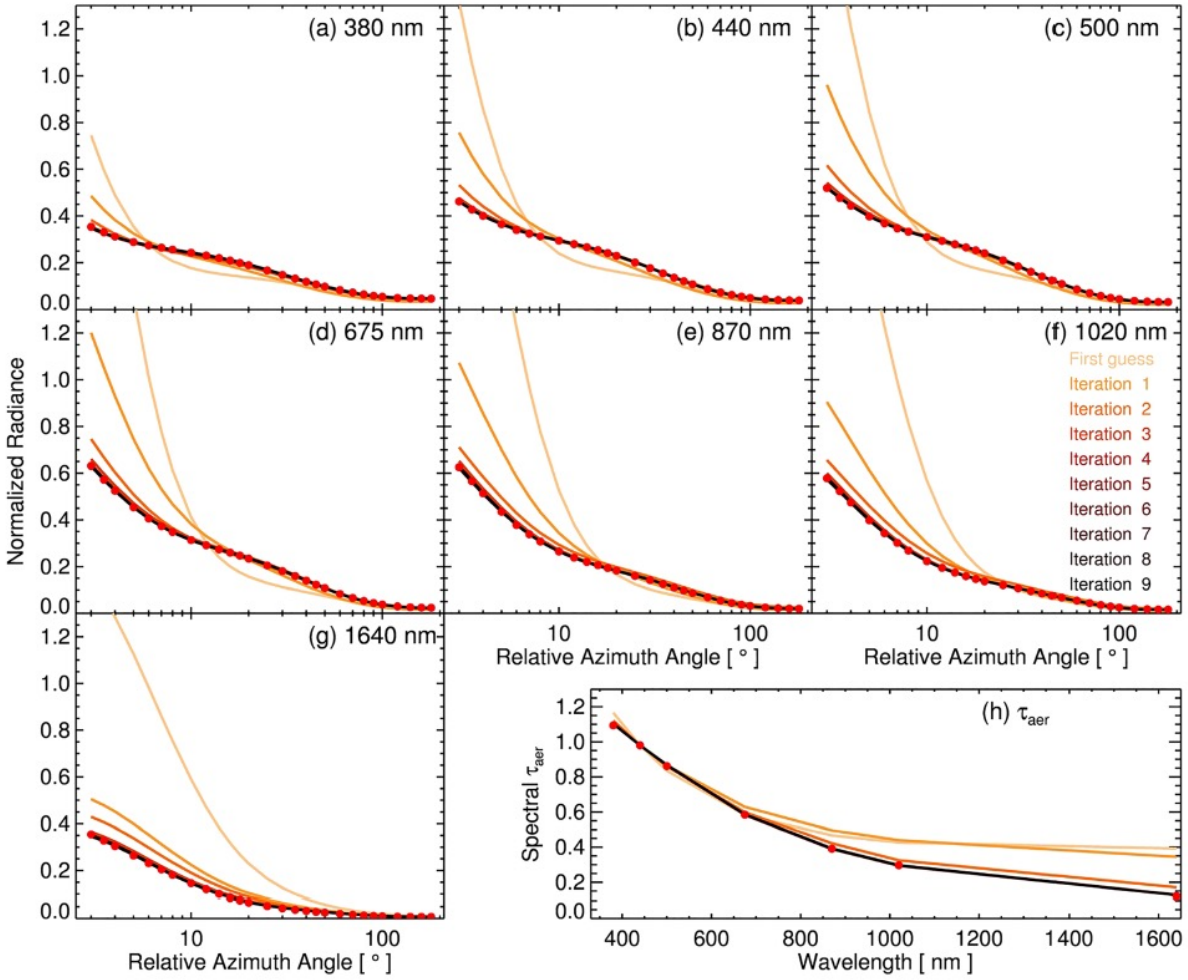

Red circle: measurements

Comparison of single scattering albedo

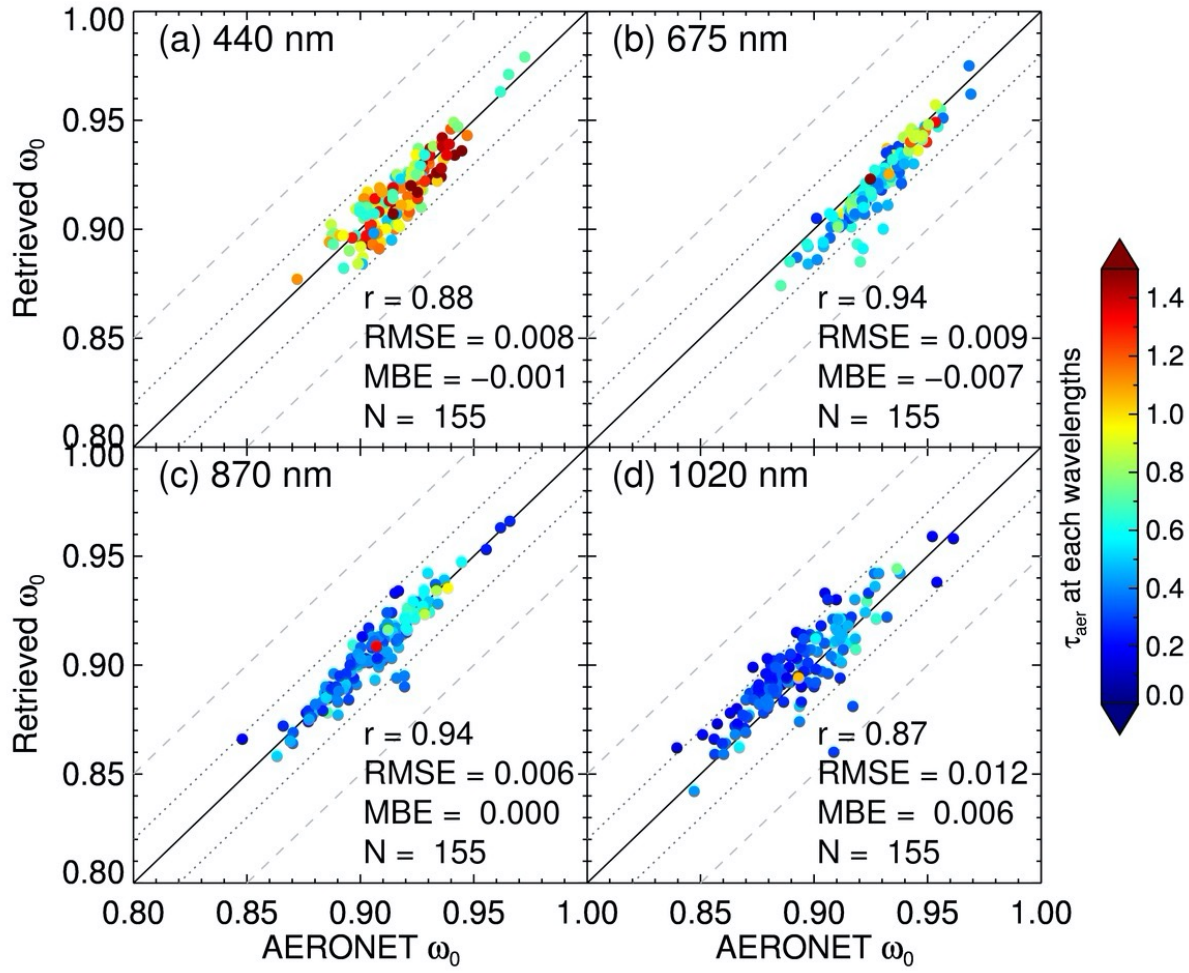

We defined successful retrieval as fitting residuals less than 2%

AERONET (Version 3, Level 2.0) direct-Sun aerosol optical depth and almucantar sky radiances measured at Kanpur, India in 2016

Consistency check with the AERONET

- The SMART-s aerosol algorithm utilizes stronger constraints of the particle-size-distribution (PSD), but less constraints for the spectral-refractive-index.
- Higher spectral resolution provides good information on fine-mode PSD, whereas longer wavelength channels of the AERONET are beneficial for coarse-mode PSD retrievals.
- Modified version of the aerosol PSD function (e.g., Kok, 2011; Zhang et al., 2013) may better reflect actual aerosol PSD, and can be implemented in the future algorithm.

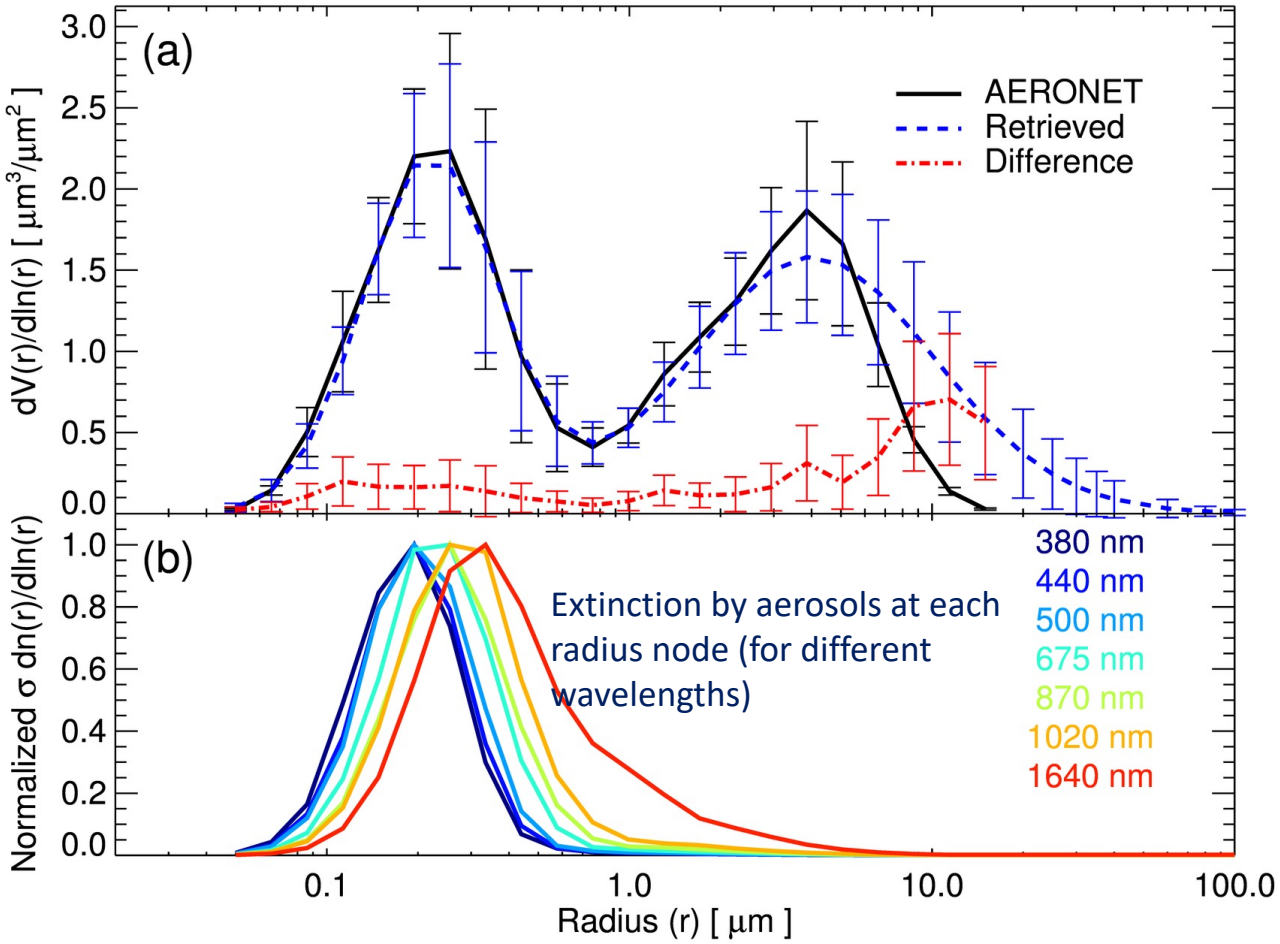

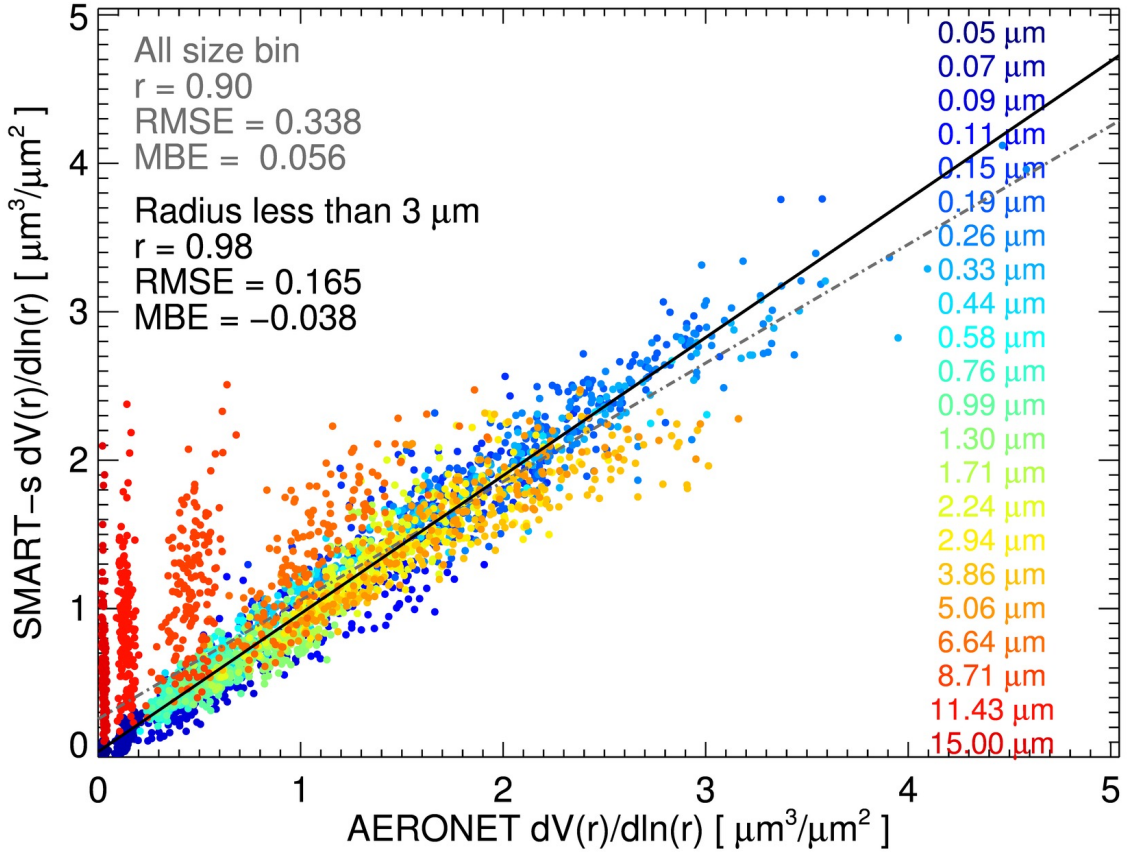

AERONET (Version 3, Level 2.0) direct-Sun aerosol-optical-thickness and almucantar sky radiances measured at Kanpur, India in 2016

Error estimations for different type of measurements

- The retrieval errors are when SMART-s algorithm was applied to different type of measurements (**AERONET-like**, **Pandora** and **SMART-s**).
- We considered three types of aerosols (sulfate, smoke, dust), SZAs from 50°-75° at 5° interval.
- The high-spectral measurement (Pandora and SMART-s) can provide informative retrievals of fine-mode aerosols, whereas Pandora measurements are less sensitive to the coarse mode due to the narrower spectral range.

Particle size distribution

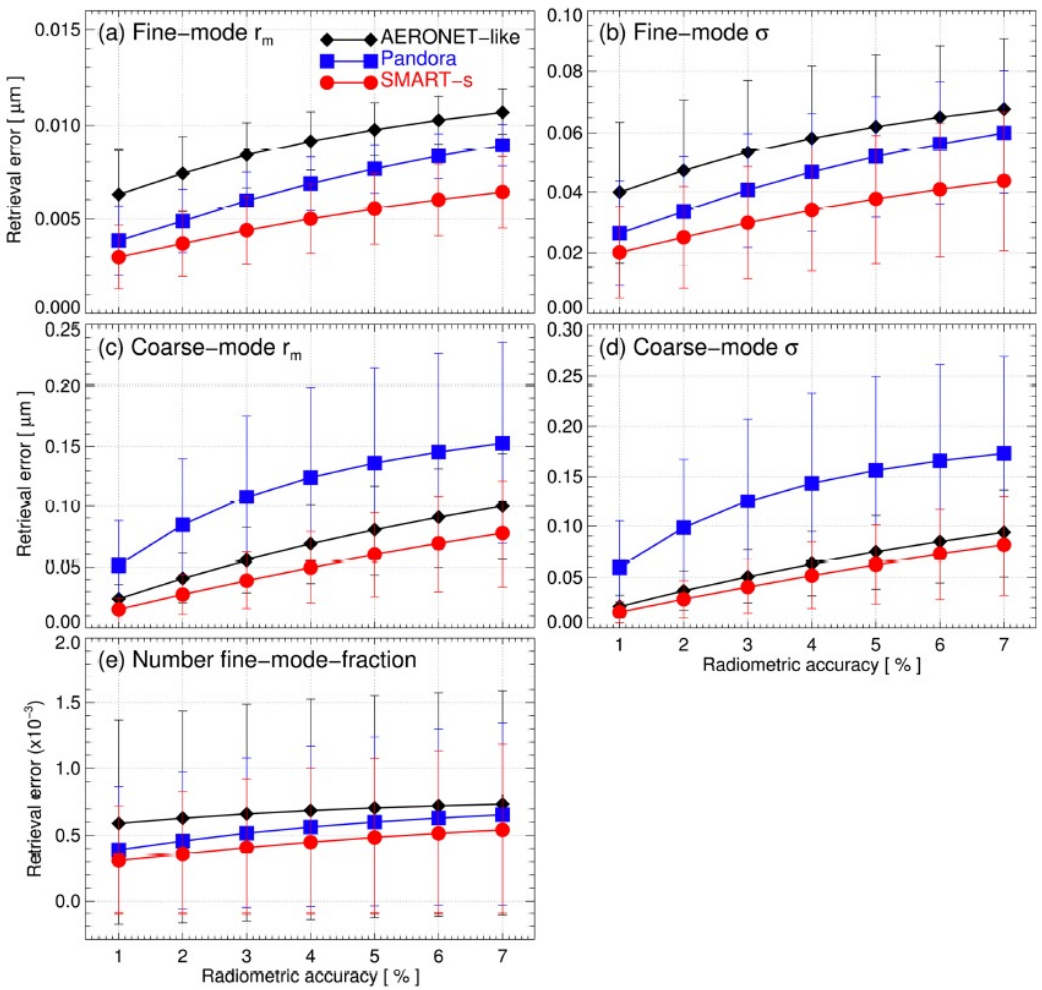

Spectral refractive index

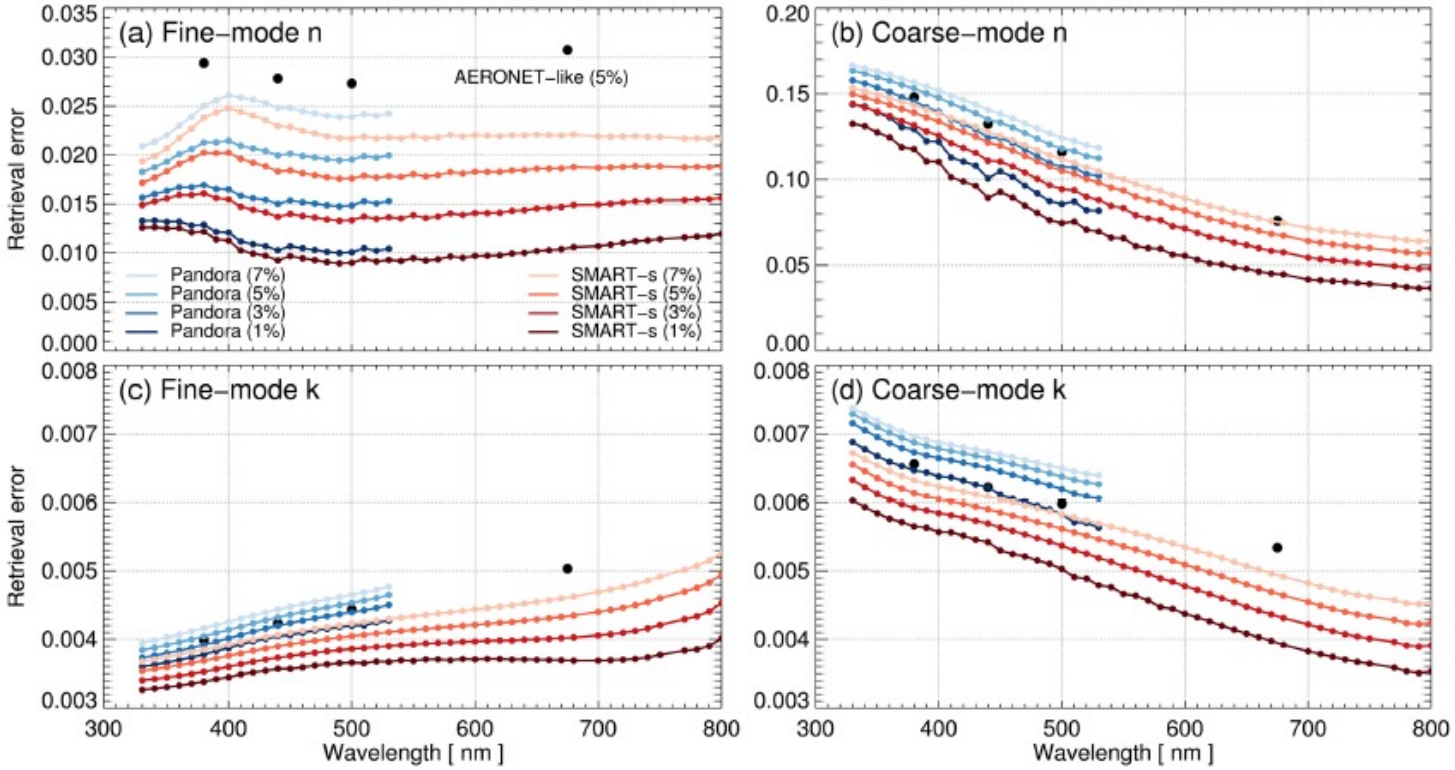

Jeong et al. (2020), *JGR-Atmosphere*

Biomass burning aerosol retrievals over Fang, Thailand

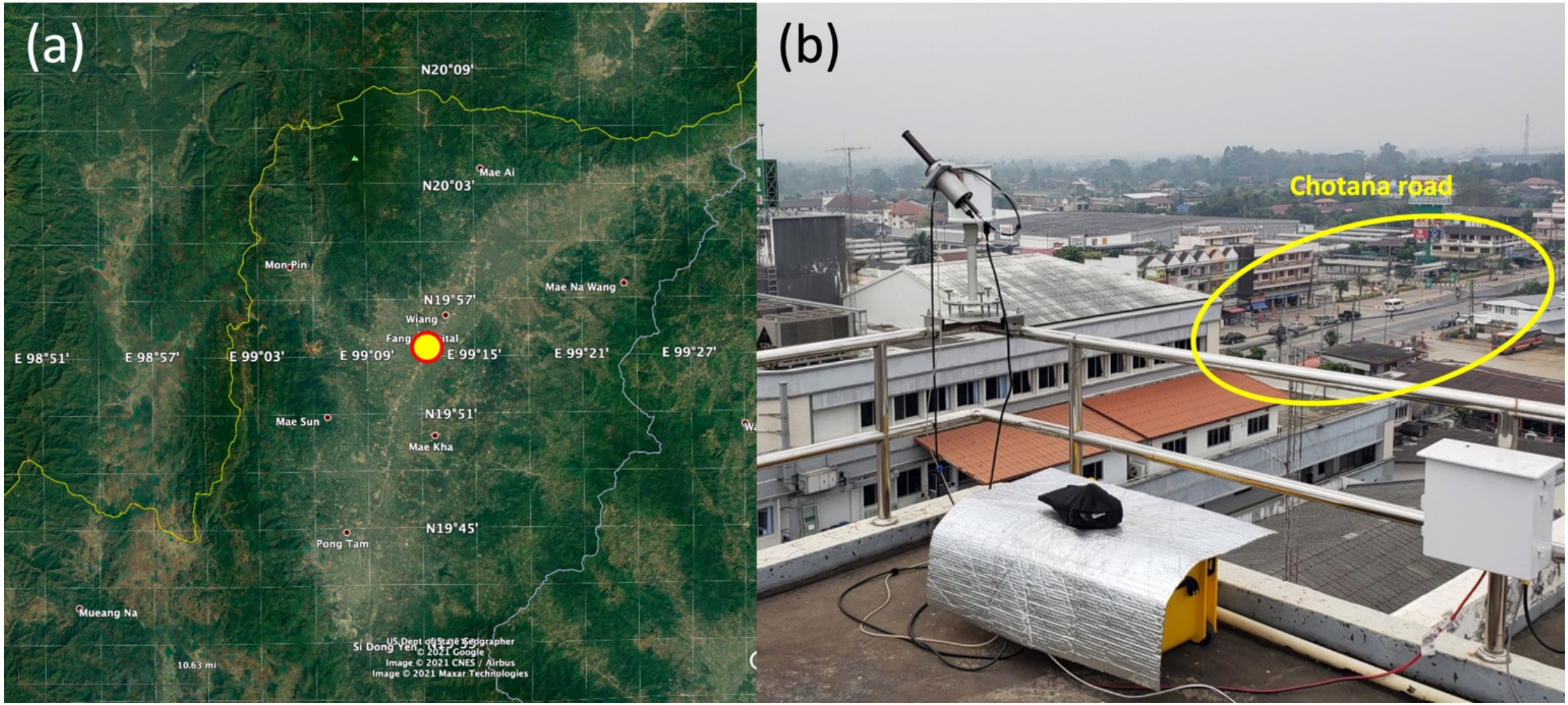

(a) Location of measurement site at the rooftop of Fang hospital, Thailand (19.91°N latitude and 99.21°E longitude, 480 m above sea level; the map is extracted from https://google.com/maps/). Panel (b) is an image of deployed SMART–s (Pandora#48) taken on 8 March 2019. The Chotana road (marked as yellow) is one of the major streets at this area, and is about 50 m away from the site.

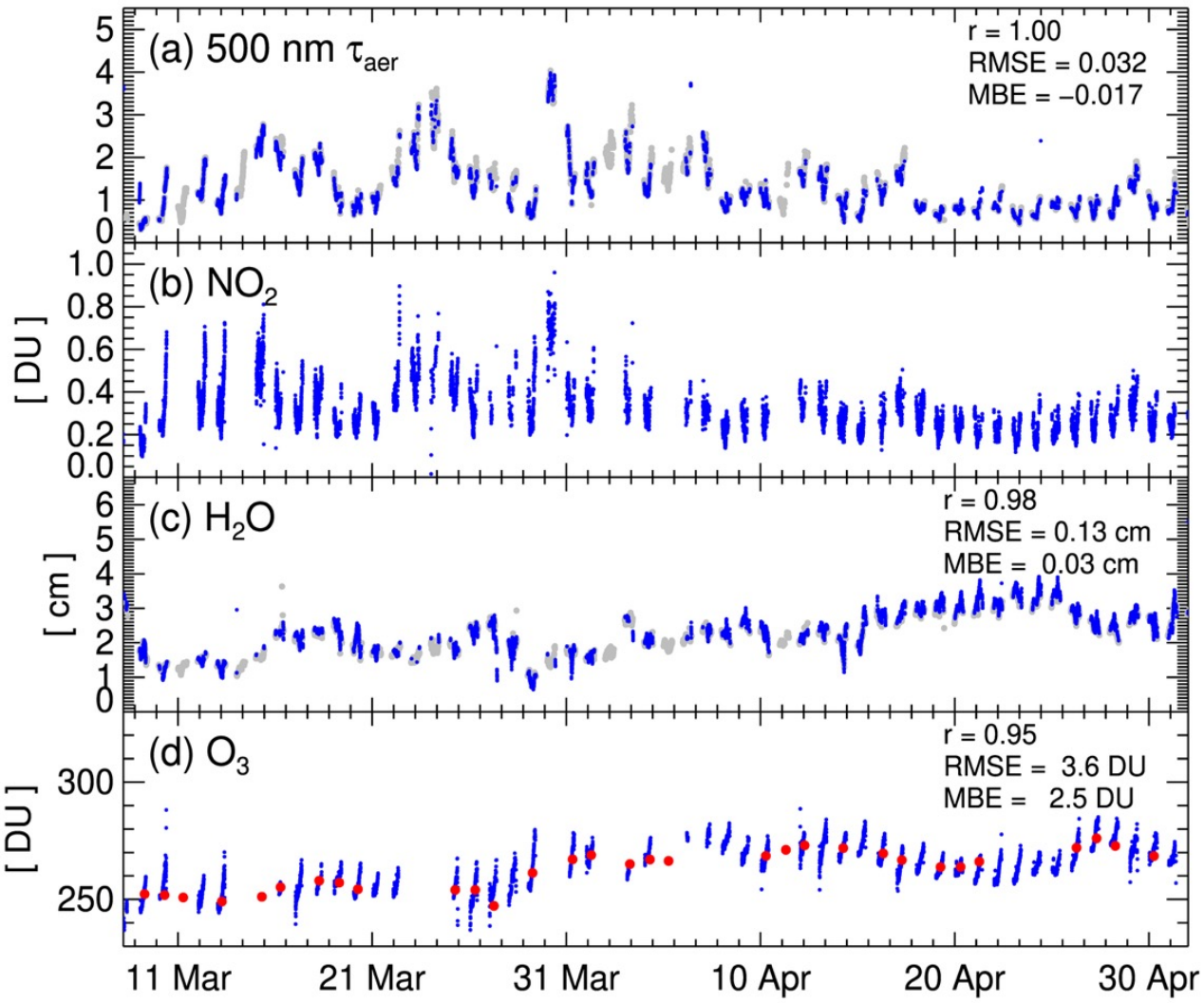

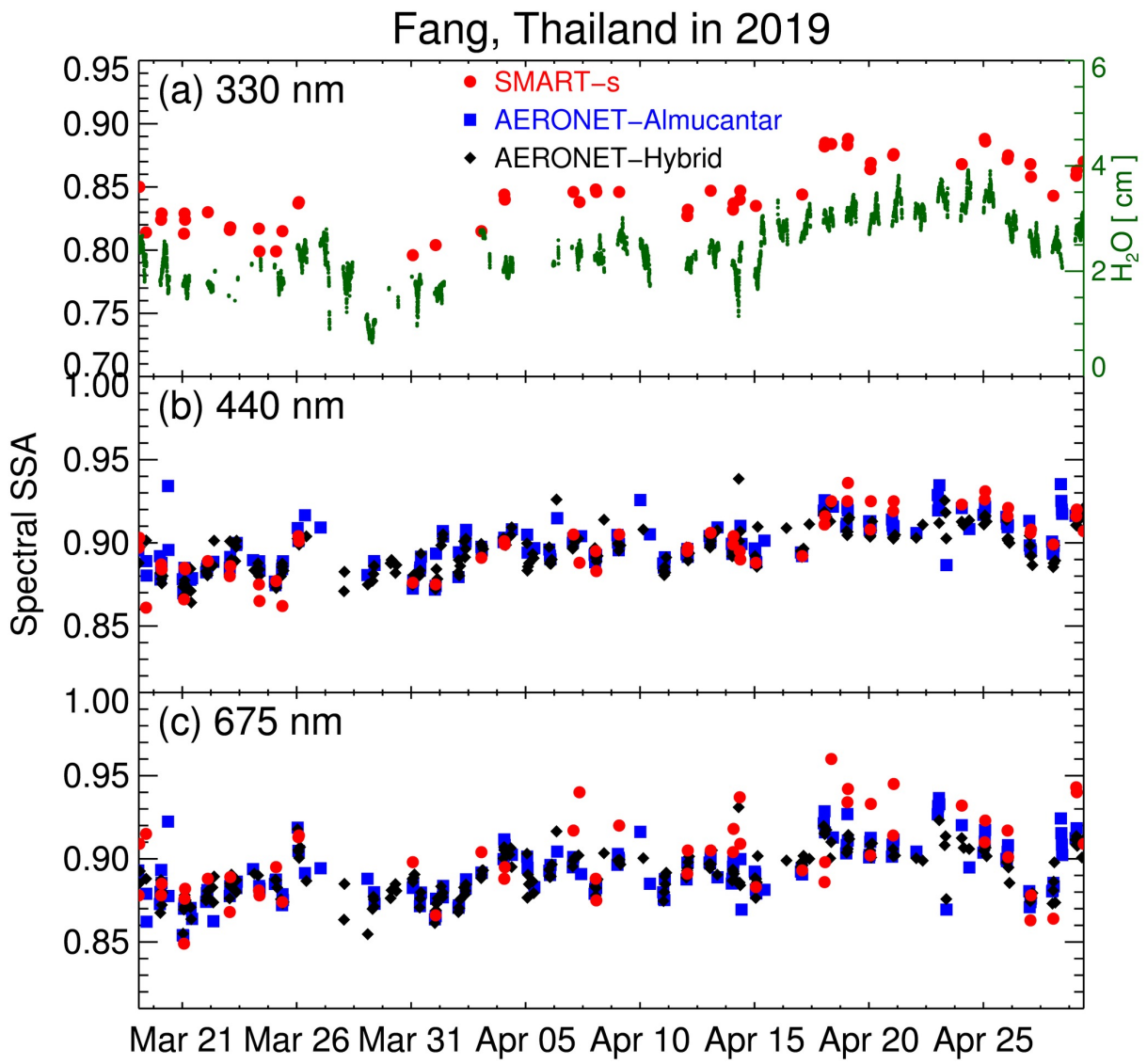

Temporal variations of total columns of (a) aerosol extinction at 500 nm, (b) nitrogen dioxide, (c) water vapor, and (d) ozone at Fang, Thailand in 2019. The blue circles are from SMART–s retrievals, and the grey circles in panel (a) and (c) shows those from the AERONET, and the red circles in panel (d) are total column ozone retrievals from OMI (TOMS Version 8.5). The correlation coefficient (r), root-mean-squared-error (RMSE), and mean-bias-error (MBE) at panel (a), (c), and (d) are between collocated SMART–s and AERONET/OMI data.

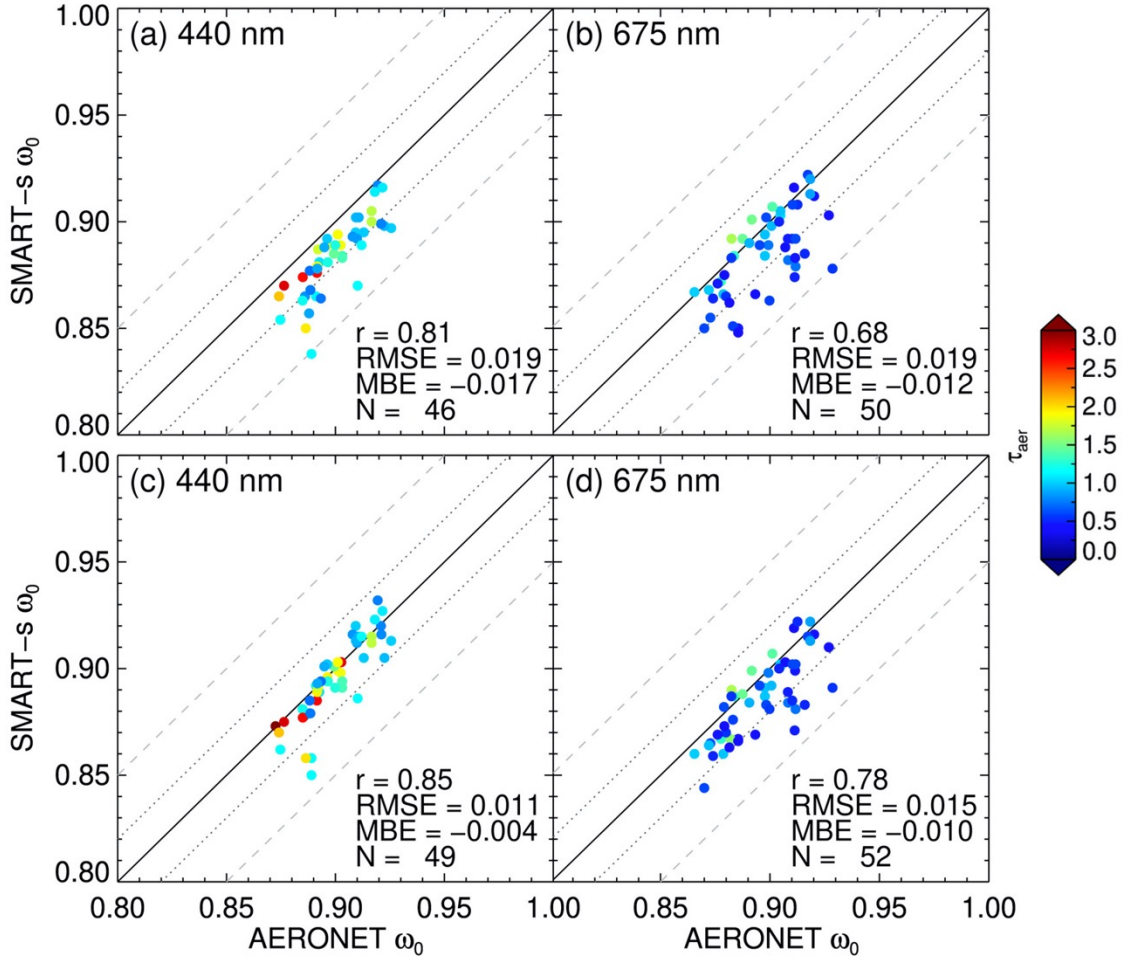

Comparison of single-scattering albedo (ω_0) from SMART-s and AERONET (Version 3, Level 2.0) at (a) 440 and (b) 675 from 19 March to 2 May 2019. In these panels, SMART–s algorithm utilized solar irradiance from Chance and Kurucz (2010). Panel (c) and (d) are similar plot but the SMART–s retrievals using derived solar irradiance in this study. Color of the circle represents aerosol optical thickness (τ_{aer}) at each wavelength. The r is the correlation coefficient, RMSE denotes root-mean-square error, and MBE is the mean-bias error, and N is the number of samples for the comparison. The dotted line and dashed line represent relative biases of ±0.02 and ± 0.05 from the AERONET product.

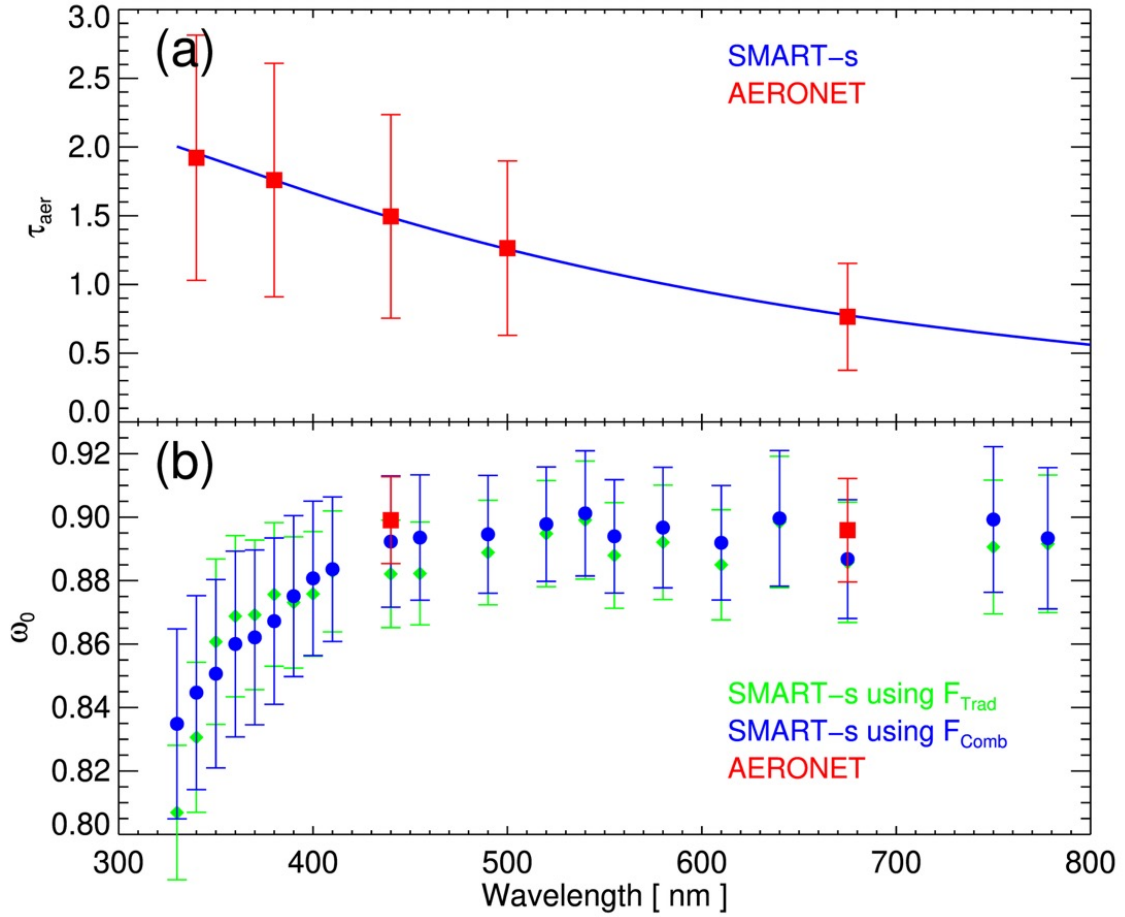

Mean values of (a) spectral aerosol optical thickness (τ_{aer}) from SMART–s (blue line) and AERONET (red square) within SMART–s spectral range measured from 8 March to 2 May 2019 at Fang, Thailand. Panel (b) shows those of spectral single-scattering albedo of aerosols (ω_0) from AERONET (red rectangle) and SMART–s using different solar irradiance; green diamonds used Chance and Kurucz (2010) and blue circles used spectrum derived in this study. Error bar in panel (a) and (b) represents standard deviation of each value during the period.

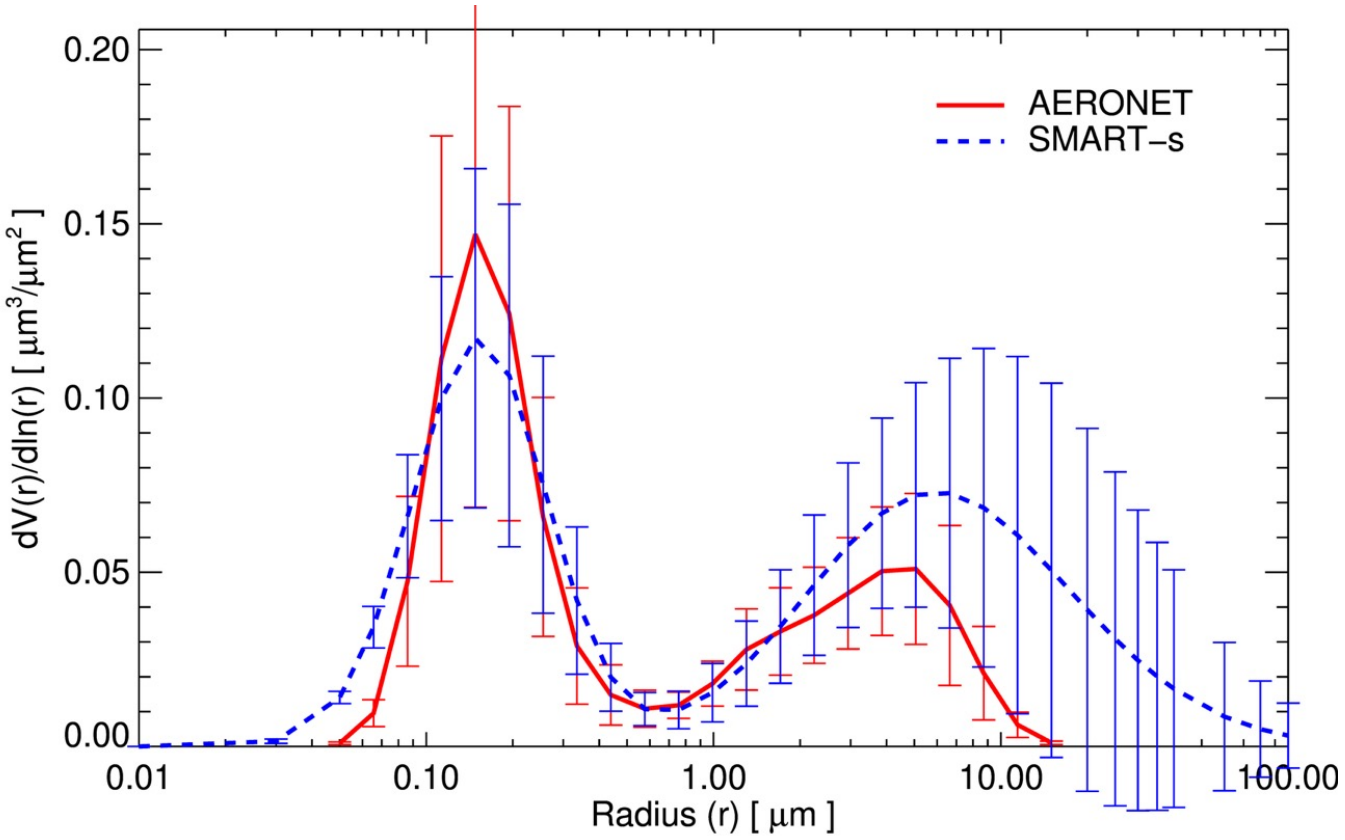

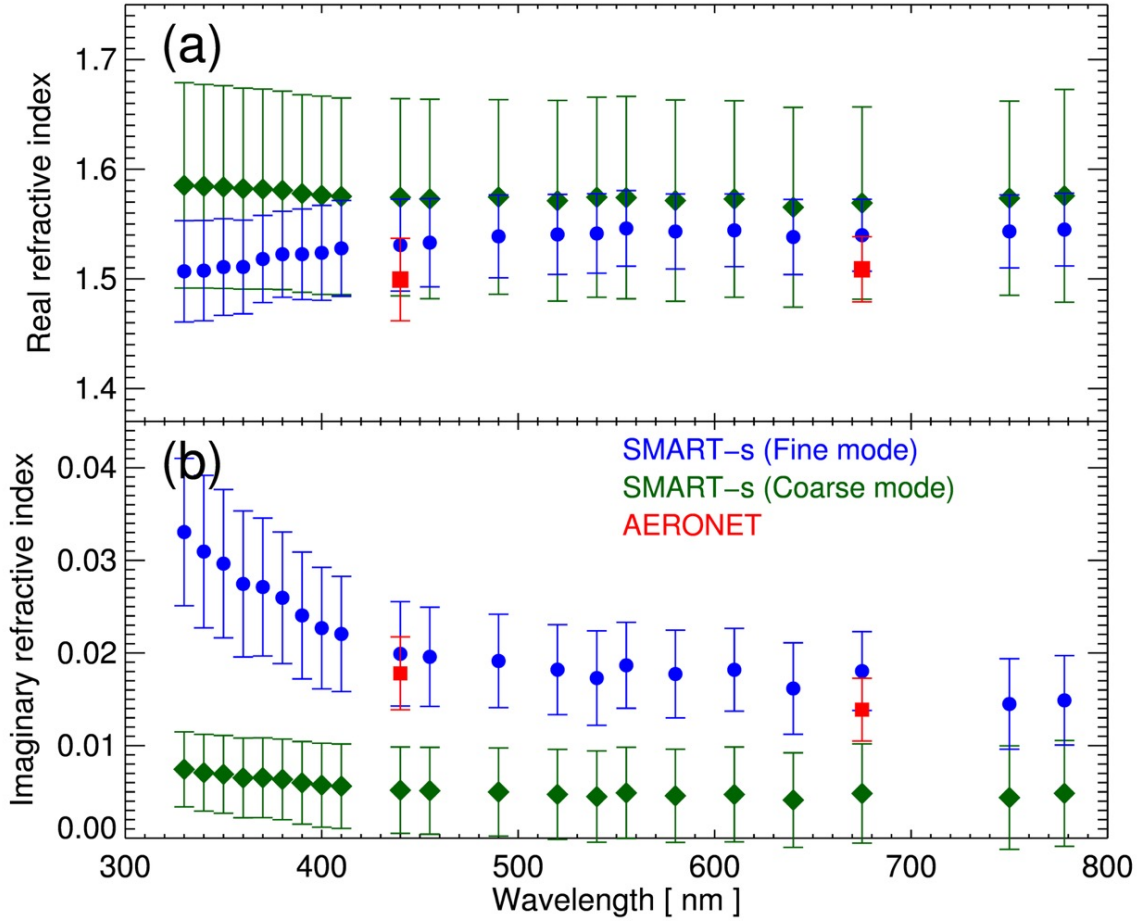

Average volume-size-distribution of aerosols retrieved from SMART–s (red solid line) and AERONET (blue dashed line) from 8 March to 2 May 2019 at Fang, Thailand. Error bar indicates their standard deviations at each radius node during the period.

Variabilities of the aerosol properties over globe?